

Reliable Shadow Area Recovery with Two-Spatial-Frequency Fringe Projections from Two Projectors

Yang Yang,¹ Wei Liu,^{*},¹ Yi Ding,² Yate Jiang,¹ Kai Peng¹

¹*School of Electronic, Information and Communications, Huazhong University of Science and Technology, 1037 Luoyu Road, Wuhan, Hubei, China*

²*Wuyi University, Jiangmen, Guangdong, China*

Keywords: Fringe projection profilometry, Three-dimensional reconstruction, Fringe analysis, Phase measurement.

Abstract: Shadow always appears on the captured fringe images in traditional fringe projection profilometry system. To recover the shadow area, in existing methods, fringe patterns from multiple projectors are employed to calculate the absolute phase maps of entire object surface. However, if the fringe order errors in the absolute phase maps were not corrected, significant errors would appear on the reconstructed three-dimensional result. In this paper we propose a method to recover the entire surface profile with the fringe projections from two projectors. In the proposed method, the shadow areas are identified, a novel technique is developed to correct the fringe order errors in the absolute phase maps of the fringe patterns from two projectors, thus the reliability of shadow area recovery could be improved. This method also can be used for various applications in industries and academics. The methodology is exemplified with experimental data.

1. INTRODUCTION

Fringe projection profilometry (FPP) is considered as a promising noncontact measuring method to obtain three-dimensional profile data in industries for product surface inspection and visual navigation for decades (R. Leach,2011)(J. Geng,2011). In FPP, a set of sinusoidal fringe patterns from micro-mirror device is generated and projected onto the surface of measured object and the light signals are captured by a CCD camera. Due to the nature of structured light illumination, shadow occurs in the capture image when the projected illumination signal is blocked by the shape of measured object. As the shadow areas of captured image hardly reflect the modulated light signals associated with object surface, the captured signals in shadow areas cannot be directly employed for three-dimensional reconstruction. To eliminate the effect of shadow areas in the captured fringe patterns, Lu et al. (L. Lu et al,2015) developed a method to determine the shadow areas by mapping the reconstruction depth result to digital micro-mirror-device plane in pixel-by-pixel manner.

The shadow areas in captured fringe image are mainly resulted from the geometry of traditional fringe projection profilometry system, if the fringe patterns from different illumination angles could cover the entire surface and their reflections are captured by camera, it is possible to recover the

entire profile data. Skydan et al. (O. A. Skydan,2005) employed the fringe images from multiple angles to obtain the entire profile 3D reconstruction result. Cai et al. (Y. Cai et al,2007)

proposed the inverse projected fringe technique based on multiple projectors to recover the shadow area more efficiently. Some methods have been developed to improve the accuracy and robustness of entire surface acquisition from multiple angles for entire shape acquisition (W. H. Su,2008)(X. Liu,2012). However, in these methods, fringe patterns of only one spatial frequency is used, errors may occur to the absolute phase maps due to the complex object surface and shadow areas. Servin et al. (M. Servin et al,2013) proposed a co-phased profilometry to convert the phase demodulation of multiple camera-projector systems into a single process. In this method, the wrapped phase extraction can be considered as an extension of the standard Fourier Transform, thus the reconstructed result is sensitive to the intensities of background illumination and projected light signal. The points of shadow areas generated by each projector may affect the reconstruction results of the areas without shadow. Furthermore, the sensitivities of the fringe patterns from multiple projectors should be the same to keep the accuracy of measurement, which is difficult to satisfy in many applications.

This paper proposes a method to improve the reliability of the 3D profile recovery in shadow areas with the two projectors in two angles. In particular, this paper focuses on the case that, for each projection, the fringe patterns generated by projector can be reflected by the object surface and are acquired by the camera. Only parts of the surface are shadow areas, which are not illuminated by the fringe pattern of projector.

The proposed method improves the reliability of the shadow area recovery as follows. The points in the shadow areas generated by each projector are identified, the corresponding wrapped phase values are labeled as invalid. For the points in the areas illuminated by each projector, the corresponding wrapped phase maps and absolute phase maps are calculated with phase-shifting algorithm and two-spatial-frequency temporal phase unwrapping, which avoids the influence of the points in shadow areas. For the possible fringe order errors in the absolute phase maps around the shadow areas, we develop a novel fringe order correction technique to correct these errors. With the proposed method, the profile of shadow areas generated by each projector can be recovered. Finally, the complete 3D profile could be obtained with high reliability.

The rest parts of this paper are organized as follows. In Section 2 we present the identification of points in shadow areas. In Section 3, reliable absolute phase recovery for the fringe patterns generated by each projector is developed. In Section 4, the method to recover the complete 3D profile is developed. In Section 5, the experiments are presented to confirm the method. Section 6 concludes the whole paper.

2. PRINCIPLE OF FPP AND SHADOW AREA IDENTIFICATION

2.1 Principle of FPP

Fig.1 shows the system structure diagram of traditional fringe projection profilometry, which includes one projector and one camera. Fringe patterns are generated and projected onto the object surface and reference plane. Camera acquires these fringe pattern images for surface profile recovery. For the area illuminated by projector, the information of surface profile is modulated into the deformed fringe pattern, thus it is possible to reconstruct the surface of object with the captured

fringe images. In existing methods, wrapped phase extraction should be implemented to obtain the information of fringe pattern for height distribution reconstruction. Among various wrapped phase extraction and phase unwrapping methods, phase shifting algorithm are the most widely used for the reliability and the avoidance of the influences from adjacent pixels, which can eliminate the effects from the points in shadow area.

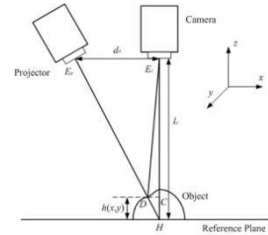


Figure 1: System structure diagram of traditional FPP.

For the N -step phase shifting algorithm, the fringe patterns captured by camera could be expressed as

$$d_n^c(x, y) = A(x, y) + B(x, y) \cos(2\pi f_0 x + \phi(x, y) + \frac{2\pi(n-1)}{N}) \quad (1)$$

where $n = 1, 2, 3, \dots, N$; $\Phi(x, y) = 2\pi f_0 x$ is the designed absolute phase map in the projector, f_0 is the spatial frequency of the fringe pattern; $A(x, y)$ denotes the average intensity, $B(x, y)$ denotes the intensity modulation of the sinusoidal fringe pattern, $\phi(x, y)$ is the wrapped phase. When $N \geq 3$, $A(x, y)$, $B(x, y)$ and $\phi(x, y)$ can be calculated as,

$$A(x, y) = \frac{1}{N} \sum_{n=1}^N d_n^c(x, y) \quad (2)$$

$$B(x, y) = \frac{2}{N} \sqrt{[\sum_{n=1}^N d_n^c(x, y) \sin(\frac{2\pi n}{N})]^2 + [\sum_{n=1}^N d_n^c(x, y) \cos(\frac{2\pi n}{N})]^2} \quad (3)$$

$$\phi(x, y) = \arctan \frac{\sum_{n=1}^N d_n^c(x, y) \sin(2\pi n / N)}{\sum_{n=1}^N d_n^c(x, y) \cos(2\pi n / N)} \quad (4)$$

Define

$$\gamma(x, y) = \frac{B(x, y)}{A(x, y)} \quad (5)$$

where $\gamma(x, y)$ denotes the data modulation, it is always used as the index to evaluate the quality of the fringe pattern (S. Zhang, 2006). Higher $\gamma(x, y)$ means the better fringe quality.

To recover the surface profile of object, phase unwrapping should be implemented to obtain the

absolute phase from wrapped ones calculated by phase-shifting algorithm in Eq.(4) . The relation between absolute phase and wrapped phase is expressed as

$$\Phi(x, y) = 2\pi m(x, y) + \phi(x, y) \quad (6)$$

where $m(x, y)$ denotes the fringe order, which is in integer, $\Phi(x, y)$ is the absolute phase. When the absolute phase maps of the fringe patterns on object $\Phi^D(x, y)$ and on reference plane $\Phi^R(x, y)$ are obtained, the difference of the absolute phase maps $\Delta\Phi(x, y)$, where $\Delta\Phi(x, y) = \Phi^R(x, y) - \Phi^D(x, y)$, is used to calculate the height distribution of the surface profile of object as:

$$h(x, y) = \frac{\Delta\Phi(x, y)l_0}{2\pi d_0 f_0} \quad (7)$$

where l_0 and d_0 are the parameters calibrated before the measurements.

2.2 Shadow Area Identification

Due to the geometry in traditional fringe projection profilometry in Fig.1, shadow always occurs in the captured images. The shadow areas in the captured images do not reflect the modulated light signal of the projected fringe patterns. When phase shifting algorithm or other wrapped phase extraction algorithm is directly used to the pixels in shadow, errors will occur in the corresponding wrapped phase value. These incorrect wrapped phase values will cause the errors in the reconstruction of the object. We use Fig.2 to illustrate the reason causing the shadow in traditional FPP system.

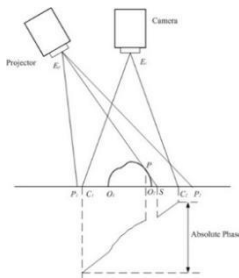


Figure 2: Shadow area formation and absolute phase of illuminated area in FPP system.

The field of view of the camera and projector is $E_c C_1 C_2$ and $E_p P_1 P_2$ respectively. The light beam $E_p P S$ emitted from the projector reaches point S

through point P on the object. Since the light beam is blocked by the object through point P , shadow area $P O_2 S$ is formed. The camera acquires the fringe patterns in another direction, so the shadow area $P O_2 S$ will be captured by the camera, which does not reflect the modulated light signal to the camera. Thus the pixels in the image acquired by camera can be divided into two types of area as the fringe pattern area and shadow area.

To identify the surface profile in shadow areas, the points in shadow can be recognized by checking whether the captured fringe patterns are from the digital micro-mirror device plane (L. Lu.,2015). Theoretically, if the points of the results calculated by phase-shifting algorithm were mapped to the digital micro-mirror device plane, the mapped points from the shadow area will be out of the boundary of digital micro-mirror device plane. Therefore the points in shadow area can be determined through this mapping. Since the wrapped phase values in shadow areas are not reliable, we label these values as invalid to distinguish from the points in the area illuminated by projector.

3. RELIABLE ABSOLUTE PHASE RECOVERY

3.1 Absolute Phase Map Recovery with Temporal Phase Unwrapping

To calculate the absolute phase and fringe order of the surface with shadow, we take one section from point C_1 to point C_2 shown in Fig.2 as an example.

C_1, C_2, O_1, O_2, P, S are used to represent the coordinates of the corresponding points on the section respectively. For simplicity, we use $\Phi(x)$ and $m(x)$ to denote absolute phase $\Phi(x, y)$ and fringe order $m(x, y)$ respectively. In Fig.2, the areas from point C_1 to point P and from point $S+1$ to point C_2 are illuminated with fringe projections, the area from point $P+1$ to point S is the shadow. Based on the shadow area identification in (L. Lu,2015), the unreliable absolute phase values in shadow from point $P+1$ to point S are also labeled as empty values. For the area illuminated by fringe projections, the point on the fringe image captured by camera is one-to-one map to the point in digital micro-mirror device plane. Therefore, when the absolute phase and fringe order in the areas illuminated by fringe projections are correctly

recovered, the absolute phase should be monotonically increasing, the fringe order should be stepwise increasing. So the absolute phase from point C_1 to point P and from point $S+1$ to point C_2 keeps monotonically increasing, we also have $\Phi(S+1) > \Phi(P)$ (S. Zhang,2006). Since the fringe order from point C_1 to point P and from point $S+1$ to point C_2 is stepwise increasing, we also have $m(S+1) \geq m(P)$ (S. Zhang,2006).

In order to recover the absolute phase map of the surface with shadow, temporal phase unwrapping is used due to its independence of the wrapped phase values of adjacent pixels. In temporal phase unwrapping, the fringe order of absolute phase is uniquely determined with selected multiple-spatial-frequency fringe projections(H. O. Saldner,1997)(Liu, Y. Wang,2010).

However, when the noise in wrapped phase map exceeds the phase error tolerance bound, errors may occur in the fringe orders recovered by temporal phase unwrapping (Y. Ding,2012)(L. Song,2014), which makes the recovered fringe order value different from its true value. To illustrate the fringe order error in the recovered absolute phase, we show an experiment results shown in Fig.3. In this experiment, we project two sets of fringes at the two normalized spatial frequencies 8 and 15 onto the measured object, the normalized spatial frequency 8 means the image is covered with 8 complete fringe, the normalized spatial frequency 15 means the image is covered with 15 complete fringes. We label the wrapped phase, fringe order and absolute phase of the points in shadow areas as invalid, which are indicated as empty in Fig.3(a) and Fig.3(b). The wrapped phase maps of the area illuminated by fringe projections are obtained with phase-shifting algorithm (X. Su,1992), the corresponding fringe orders are recovered with temporal phase unwrapping method in (Y. Ding, 2011). The recovered fringe order and absolute phase and of section $y=690$ at the normalized spatial frequency 15 are shown in Fig.3 as follows.

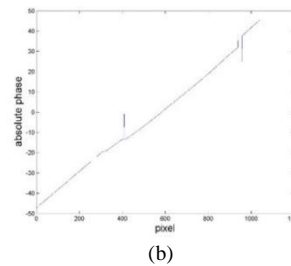
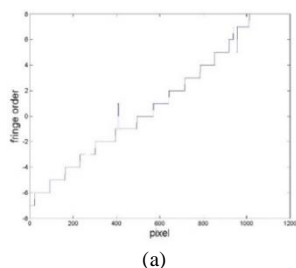


Figure 3: The recovered fringe order (a) and the recovered absolute phase (b) of section $y=690$ at the normalized spatial frequency 15.

From Fig. 3, we notice that few points are with fringe order errors in the area illuminated by fringe projections, thus it is necessary to correct these errors for high reliable temporal phase unwrapping.

3.2 Fringe Order Error Correction for the Absolute Phase Separated by Shadow Areas

For the surface without shadow, some methods find and amend the fringe order errors by checking the numerical difference of the calculated absolute phase values between neighbor pixels (H. Wang,2015)(C. Zhang,2015) or designing the filter window size according to this difference (D. Zheng,2017). Since the absolute phase and the fringe order of the area illuminated by fringe projections are separated into several intervals by shadow areas, these correction methods cannot be used for the surface with shadow areas.

To correct the fringe order errors occurring in the absolute phase map separated by shadow areas, we have the discussion as follows. According to the physical meaning of fringe order, the section of fringe order map is divided into some steps by the fringe projections, the fringe order values of the points in each step should be the same. The bounds of steps can be found by checking the phase discontinuities in wrapped phase map, the bounds of shadow areas are also considered as the bounds of step. The diagram of step division is shown in Fig.4.

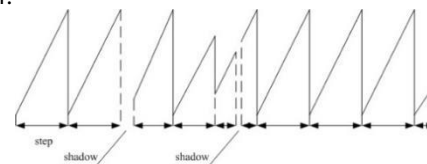


Figure 4: Step division separated by shadow area.

Thus when the fringe order values of the pixels in one step are not the same, the fringe order error must occur in this step. Since the noise in temporal phase unwrapping can be modeled as Gaussian distribution with the mean as the true fringe order value (Y. Ding, 2017), thus most of the fringe order values of the pixels in each step recovered by temporal phase unwrapping will be correct, experimental results in many references confirm this inference. Based on this inference, we can find that in each step, it is high probability that the fringe order value with the most pixels is the true fringe order of this step. We consider this fringe order value as the true fringe order of this step, the fringe order values of the pixels in this step are all replaced by this value.

If the fringe order value with the most pixels is not the true fringe order, this processing can reduce the random fringe order errors into the same wrong fringe order value. The fringe order error is in integer, thus the absolute phase error is in the times of 2π . This kind of fringe order error can be found by checking the difference of the absolute phase values in this step with the nearest two steps. Along the x -axis, one of the nearest two steps is on the right side of this step, the other is on the left side of this step. When this error occurs, the difference of the absolute phase values will exceed π , the increase and decrease of absolute phase will appear in pair as in Fig.3(b).

Therefore, for the surface with shadow, we can summarize the technique to correct the fringe order error of the absolute phase separated by the shadow area as follows:

1. On the fringe order map recovered with temporal phase unwrapping, divide the section of fringe order map into several intervals row by row based on the phase jump and bounds of shadow areas in wrapped phase as Fig. 4., each interval corresponds to one step.

2. Count the number of pixels for every fringe order value in each step. If the fringe order value of one step keeps the same, the fringe order value is judged as true fringe order value of this step.

3. For the step with multiple fringe order values, find the fringe order value with the most pixels. This fringe order value is judged as the true fringe order value, the other fringe order values are replaced by this value.

4. Mark the steps corrected in Step 3. Compare the absolute phase values on the bounds of these steps with the absolute phase values on the bounds of the two nearest steps. In the two nearest steps, one is on the right side of the corrected step, the

other is on the left side of the corrected step. When the increase of the absolute phase values on the bounds of the two nearest steps exceeds π and the decrease of the absolute phase values on the bounds of the two nearest steps is less than $-\pi$, we can judge the fringe order value of the corrected step as wrong. If such pair appears, we discard the absolute phase values in the corresponding step since they are not reliable. If there is no such pair, it means the fringe orders are correctly fixed.

By this technique, we can detect and correct the fringe order errors of the area illuminated by fringe projections. Thus, the height distribution of such area can be corrected with high reliability.

4. SHADOW AREA RECOVERY WITH TWO PROJECTORS

From the discussion in Section 2, we can see that the shadow area is formed when the illumination signal emitted by projector is blocked by object surface. To recover the surface profile in shadow areas, information of fringe pattern in these areas should be added. Based on this consideration, we design a fringe projection profilometry system with two projectors and one camera, the two projectors are on the two sides of camera. For the objects with convex surface profile, two projectors could cover the entire surface. The diagram of this system is shown in Fig.5.

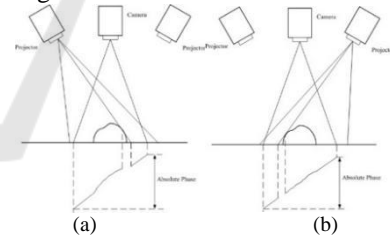


Figure 5: FPP system with two projectors and one camera.

In Fig.5(a) and Fig.5(b), the shadow area formed by the left projector can be illuminated by the right projector, the shadow area formed by the right projector can be illuminated by the left projector. The object is illuminated by the fringe patterns emitted by two projectors sequentially. By this design, the shadow area from one projector can be illuminated by another projector. The positions of two projectors are on the symmetry of camera.

From the discussion in Section 3, we infer that the possible errors in recovered fringe order values

could be corrected by the monotonic property of absolute phase. Therefore, we design the projections from the left projector as its true absolute phase monotonically increasing along the x -axis, the height distribution of can be obtained. The projections from the right projector are similar, the height distribution the area illuminated by the fringe projection from left projector can be obtained. The 3D profile of the shadow areas generated by one projector can be recovered with the reliable absolute phase of the fringe projections generated by another projector, the complete three-dimensional reconstruction result of object can be obtained. For areas illuminated by two projectors, we can decide which height value is used for 3D profile reconstruction based on the quality evaluation of fringe projection in Eq.(5).

We summarize the procedures to recover the 3D profile of shadow area as:

1. Fringe patterns are casted onto the object from two projectors sequentially as Fig.5 and make sure that the shadow area generated by one projector is covered by another one. For each projector, two-spatial-frequency fringe patterns are casted. The fringe projections from two projectors are designed as Fig.5(a) and Fig.5(b) respectively.

2. For each projector, the points in the shadow areas are identified by the method in Section 2.2, which is proposed in [3], the wrapped phase values of these points are labeled as empty. The wrapped phase maps of the areas illuminated by fringe projections are obtained by phase-shifting algorithm.

3. For each projector, the absolute phase maps of the areas illuminated by fringe projections are obtained with temporal phase unwrapping. The fringe order errors in the recovered absolute phase maps are corrected by the novel technique developed in Section 3.2.

4. The complete 3D profile data are reconstructed with the corresponding reliable absolute phase maps of the fringe projections from two projectors by Eq.(7). For the areas illuminated by two projectors, we decide which height value is used based on the quality evaluation of fringe projection with Eq.(5).

5. EXPERIMENTS

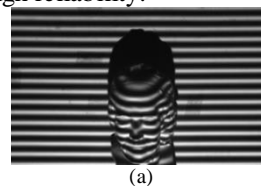
To exemplify the performance of the proposed method, experiment is implemented. The purpose of experiment is to show the proposed method could recover the entire surface correctly. The test object

is a plaster model (Voltaire, the maximal z -axis direction depth is $130mm$), the shadow areas will occur when these objects are illuminated by fringe projections. The rich detailed of object surface is suitable to illustrate the proposed method. Our experiment system is set up with two projectors and one camera, the experiment system is shown in Fig.5. The camera in the experiments is Basler MV-CS30G with its highest resolution 1296×966 , the resolution of camera can be adjusted. The projector is Acer H65010BD.

We use the fringe projection profilometry system shown in Fig.5 to capture the fringe images from the two projectors. The captured image is composed of 648×480 pixels. For each projector, we project the fringe image of two normalized spatial frequencies 8 and 15 onto the objects.

The fringe images from two projectors are shown in Fig.6(a) and Fig.6(c). In these images, we find some areas do not reflect the modulated light signal to camera, which are formed as the shadow area. The wrapped phase maps of the fringe projections from two projectors are calculated by phase shifting algorithm for noise reduction. The shadow points can be found by the method in [3], thus the wrapped phase values of shadow areas are labeled as invalid. For the areas without shadow, the absolute phase maps of these fringe projectors the two projectors are obtained by the temporal phase unwrapping developed in [22]. The fringe order errors in absolute phase maps are corrected by the technique described in Section 3.2, the corrected absolute phase maps of the fringe patterns of two projectors are shown in Fig.6(b) and Fig.6(d). The absolute phase values in shadow areas are also labeled as invalid, showing as the white parts in Fig.6(b) and Fig.6(d) respectively.

With these absolute phase maps, we can obtain two partial 3D reconstruction results. The complete 3D reconstruction result is obtained with the process in Section 4, the entire three-dimensional reconstruction result is shown in Fig.6(e), the unit of depth data in z -axis direction is mm . We can see the most parts of shadow areas in Fig.6(a) and Fig.6(c) are recovered in Fig.6(e), there is no fringe order error in the complete 3D reconstruction results, thus the proposed method can recover the shadow areas with high reliability.



(a)

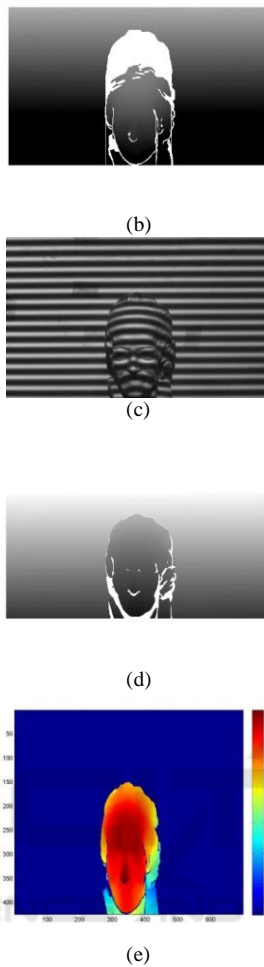


Figure 6: (a) Fringe image from lower projector. (b) Corrected absolute phase map of (a). (c) Fringe image from higher projector. (d) Corrected absolute phase map of (c). (e) Complete reconstructed 3D profile.

6. CONCLUSION

This paper develops a method for entire surface three-dimensional reconstruction with improved fringe projection profilometry. To add fringe information onto the shadow area, two projectors at symmetrical positions are used to illuminate the object surface. For the area illuminated by each projector, points in shadow areas are identified, phase-shifting algorithm and temporal phase unwrapping are employed to avoid the influence of the points in shadow area. The possible fringe order errors in recovered absolute phase map are corrected with the mathematical characteristics of

fringe order. Thus the 3D profile of shadow area for one projector can be reconstructed by the fringe projections from another projector with high reliability. The method developed in this paper can be applied to obtain entire surface profile for industrial applications.

REFERENCES

- R. Leach, *Optical Measurement of Surface Topography*, 1st. Edition, (Springer, 2011).
- J. Geng, "Structured-light 3D surface imaging: a tutorial," *Advances in Optics and Photonics*, **3**, 128-160 (2011).
- L. Lu, J. Xi, Y. Yu, Q. Guo, Y. Yin, and L. Song, "Shadow removal method for phase-shifting profilometry," *Applied Optics*, **54**, 6059-6064 (2015).
- O. A. Skydan, M. J. Lalor, and D. R. Burton, "Using coloured structured light in 3-D surface measurement," *Optics and Lasers in Engineering*, **43**, 801-814 (2005).
- Y. Cai, and X. Su, "Inverse projected-fringe technique based on multi projectors," *Optics and Lasers in Engineering*, **45**, 1028-1034 (2007).
- W. H. Su, C. Y. Kuo, C. C. Wang, and C. F. Tu, "Projected fringe profilometry with multiple measurements to form an entire shape," *Optics Express*, **16**, 4069-4077 (2008).
- X. Liu, X. Peng, H. Chen, D. He, and B. Z. Gao, "Strategy for automatic and complete three-dimensional optical digitization," *Optics Letters*, **37**, 3126-3128 (2012).
- M. Servin, G. Garnica, J. C. Estrada, and A. Quiroga, "Coherent digital demodulation of single-camera N-projections for 3D-object shape measurement: Co-phased profilometry," *Optics Express*, **21**, 24873-24878 (2013).
- S. Zhang and P. Huang, "Novel method for structured light system calibration," *Optical Engineering*, **45**, 083601 (2006).
- H. O. Saldner and J. M. Huntley, "Temporal phase unwrapping: application to surface profiling of discontinuous objects," *Applied Optics*, **36**, 2770-2775 (1997).
- K. Liu, Y. Wang, D. L. Lau, Q. Hao and L. G. Hassebrook, "Dual-frequency pattern scheme for high-speed 3-D shape measurement," *Optics Express*, **18**, 5229-5244 (2010).
- Y. Ding, J. Xi, Y. Yu, W. Cheng, W. Wang and J. Chicharo, "Frequency selection in absolute phase maps recovery with two frequency projection fringes," *Optics Express*, **20**, 13228-13251 (2012).
- L. Song, Y. Chang, Z. Li, P. Wang, G. Xing, and J. Xi, "Application of global phase filtering method in multi frequency measurement," *Optics Express*, **22**, 13641-13647 (2014).

- X. Su, W. Zhou, G. von Bally, and D. Vukicevic, "Automated phase-measuring profilometry using defocused projection of a Ronchi grating," *Optics Communications*, 94, 561-573 (1992).
- Y. Ding, J. Xi, Y. Yu and J. Chicharo, "Recovering the absolute phase maps of two fringe patterns with selected frequencies," *Optics Letters*, 36, 2518-2520 (2011).
- H. Wang, Q. Kemao, and S. H. Soon, "Valid point detection in fringe projection profilometry," *Optics Express*, 23, 7535-7549 (2015).
- C. Zhang, H. Zhao, and L. Zhang, "Fringe order error in multifrequency fringe projection phase unwrapping: reason and correction," *Applied Optics*, 54, 9390-9399 (2015).
- D. Zheng, F. Da, Q. Kemao, and H. S. Seah, "Phase-shifting profilometry combined with gray-code patterns projection: unwrapping error removal by an adaptive median filter," *Optics Express*, 25, 4700-4713 (2017).
- Y. Ding, K. Peng, L. Lu, K. Zhong and Z. Zhu, "Simplified fringe order correction for absolute phase maps recovered with multiple-spatial-frequency fringe projections," *Measurement Science and Technology*, 28, 025203 (2017).

